Longer-scale segmental dynamics of amorphous poly(ethylene oxide)/poly(vinyl acetate) blends in the softening dispersion

ARTICLE *in* SOFT MATTER · JANUARY 2011

Impact Factor: 4.03 · DOI: 10.1039/C0SM00633E

4 AUTHORS, INCLUDING:

Xuebang Wu
Chinese Academy of Sciences
43 PUBLICATIONS **249** CITATIONS
SEE PROFILE

C. S. Liu
Chinese Academy of Sciences
153 PUBLICATIONS **910** CITATIONS
SEE PROFILE

Longer-scale segmental dynamics of amorphous poly(ethylene oxide)/poly(vinyl acetate) blends in the softening dispersion

Xuebang Wu,* Huaguang Wang, Changsong Liu and Zhengang Zhu

Received 6th July 2010, Accepted 5th October 2010
DOI: 10.1039/c0sm00633e

To study the influence of poly(ethylene oxide) (PEO) on the relaxation process of poly(vinyl acetate) (PVAc) in the glass to rubber softening dispersion, the mechanical loss behaviour of PEO/PVAc blends (with PEO contents up to 20 wt%) were measured as a function of temperature and frequency. It is shown that the PEO component has a plasticizing effect on the α and α' relaxation modes of PVAc, where the α mode is ascribed to the local segmental mode and the α' mode is related to the motion of longer chain segments in the softening dispersion, composed of the sub-Rouse modes and the Rouse modes. Both the α and α' modes shifted to lower temperatures with increase of PEO concentration. Time–temperature superposition breaks down for PEO/PVAc blends in the entire temperature range due to the different friction coefficients of the α and α' modes. A single master curve of the α' mode for pure PVAc and the PEO/PVAc blends is obtained, suggesting that the size of chain segments containing on the order of 10 to 50 or more backbone bonds does not change upon blending. Furthermore, the dynamics of the α' mode of the PVAc component in the blends is found to show a characteristic crossover through the temperature dependence of relaxation time and relaxation strength. The crossover temperature T_B decreases with increasing PEO content, while the crossover relaxation time for the blends is constant with a value about 0.08 s, much longer than $10^{-7\pm1}$ s for the α mode. According to the coupling model, the crossover is suggested to be due to the variation of intermolecular coupling at T_B.

Introduction

Component dynamics in miscible polymer blends has received considerable experimental and theoretical interest not only from a fundamental point of view, but also for technological applications.[1–7] In past years, significant effort has been given to the understanding of how the segmental dynamics of each component changes upon blending.[5–10] The miscible blends are often statically homogeneous but dynamically heterogeneous, leading to a broad segmental relaxation and failure of time–temperature superposition (TTS).[10] At any given temperature, the relaxation of the high glass transition temperature (high-T_g) component in the blend is faster than the neat polymer, whereas that of the low-T_g component is slowed down upon blending.[11,12] Theoretically, many models were used to interpret these observations, such as concentration fluctuation (CF) based models, self-concentration (SC) based models, and the coupling model.[7] The CF models are based on the idea that the local concentration fluctuations are quasi-stationary near the glass transition of the blend. Fischer *et al.* developed the first model based on CF,[13,14] followed by other contributions from Kumar, Colby and co-workers.[11,15–18] The Lodge–McLeish (LM) model is one approach based on the SC effect (*i.e.* the enhanced local concentration due to chain connectivity).[4,19,20] The coupling model (CM) considers not only the presence of different local environments due to CF but also the change of intermolecular coupling due to the presence of the other component.[21] Recently, a few models that combine SC and CF effects were proposed to describe the segmental dynamics in polymer blends.[22–24]

On the other hand, the main transition of amorphous polymers from glass to rubber softening dispersion usually involves different modes of molecular motion, including local segmental motion, sub-Rouse modes and Rouse modes.[25–29] The sub-Rouse modes are immediate in both length- and time-scale between the local segmental motion and the Rouse modes. They were proposed and observed in polyisobutylene (PIB) some time ago.[26–28] The sub-Rouse modes involve segments larger than the couple of conformers involved in local segmental relaxation, whereas they contain fewer chain units than the shortest Gaussian sub-molecules described by the Rouse modes. On the other hand, the motion of the sub-Rouse modes is slower than local segmental motion due to chain connectivity but still faster than the entropically driven Rouse modes.[30] As far as the longer-scale dynamics (sub-Rouse modes, Rouse modes, *etc.*) is concerned, the CM could describe the experimental results of sub-Rouse modes since they follow the local segmental mode and have a smaller intermolecular coupling than that of the local segmental mode,[28] while the model, extended to include mitigation of lateral constraints, has also considered the terminal relaxation.[29] Based on additional assumptions beyond those used to predict segmental dynamics, the LM model is also applicable to terminal dynamics.[4] In addition, the modified tube model has been applied to describe the terminal relaxation behavior, where the friction coefficients of the Rouse segments of the component chains are evaluated on the basis of the SC concept.[10] Although the dynamics of miscible polymer blends, in general, has been widely investigated over the past years from both the experimental and the theoretical point of view, the underlying mechanism responsible for dynamics in these

Key Laboratory of Materials Physics, Institute of Solid State Physics, Chinese Academy of Sciences, P.O. Box 1129, Hefei, Anhui, People's Republic of China. E-mail: xbwu@issp.ac.cn

systems remains poorly understood, especially for the longer-scale dynamics of the components.

Mechanical spectroscopy probes the relaxation behaviors of soft matter such as polymers and biological matter over a large temperature and frequency scale.[31–34] It has proven to be useful to characterize the local segmental and longer-scale dynamics of amorphous polymers near and above T_g.[35] The mechanical loss of a material results from conformational changes leading to a phase shift between stress and strain during periodic excitation and a damping of a free vibration sample. Damping reaches its maximum when the period of molecular motion approaches the time scale of the experiments. The mechanical loss peaks and loss modulus peaks are used to pinpoint different relaxation processes, such as the local segmental motion, the sub-Rouse modes and Rouse modes.[26] It was reported that the mechanical loss peak mainly reflects the sub-Rouse modes and Rouse modes, while the loss modulus peak and the point where the storage modulus begins to drop mainly reflect the motion of local segments.[36,37]

In this work, we address the dynamics of the miscible blend of poly(ethylene oxide) and poly(vinyl acetate) (PEO/PVAc) by mechanical spectroscopy. PEO/PVAc is a very unusual blend system as it is characterized by a very large difference in the component T_g, T_g(PVAc) $\approx$ 314 K, T_g(PEO) $\approx$ 221 K.[38,39] This system has been studied recently by dielectric and viscoelastic measurements[40] revealing a single α relaxation peak which mainly reflected the local segmental motion of PVAc in the blends. In addition, TTS principle did not hold since the two components have different shift factors. A recent quasielastic neutron scattering (QENS) study showed that contrary to the low-T_g component PEO, the high-T_g component PVAc behaves in a "standard" way upon blending and the local segmental dynamics can be explained by the LM model.[39] Moreover, the microstructure and dynamics of semicrystalline PEO/PVAc blends with high PEO content were investigated by using small-angle X-ray scattering.[41] On the other hand, the dynamics of PEO in the PEO/PVAc blends have also been studied by deuterium NMR and QENS measurements,[20,38] showing that the PEO dynamics are about 9 orders of magnitude faster than the PVAc dynamics at the blend T_g and a crossover temperature was found where the dynamics of PEO change qualitatively from glass-forming polymer-like to confined.

Most previous studies about PEO/PVAc blends focused on the local segmental dynamics. As far as we know no detailed studies on the longer-scale segmental dynamics of the sub-Rouse modes and the Rouse modes in this blend have been reported so far. Here we report measurements of longer-scale segmental dynamics of the PVAc component in amorphous miscible blends with PEO using mechanical spectroscopy. Due to miscibility and PEO crystallization problems, the study of the blends is restricted to compositions with less than 20 wt% PEO.[38,39] The purpose of this work is to study how the longer-scale segmental dynamics of the PVAc component is affected by mixing with PEO, contributing to the understanding of this issue.

Experimental

The PVAc ($M_w = 5 \times 10^4$, $M_w/M_n = 1.8$) and PEO ($M_w = 1 \times 10^5$, $M_w/M_n = 1.5$) were purchased from Alfa Aesar. The molecular weight of PVAc was above the critical molecular weight ($M_c \approx 24\,500$) for chain entanglement.[25,42,43] Blends with compositions of 5/95, 10/90, and 20/80 (in wt%) (PEO/PVAc) were prepared by solution casting in a common solvent (chloroform). The films were kept in a vacuum oven for 1 week at room temperature to ensure the removal of the solvent without producing bubbles in the samples. The glass transition temperatures of the homopolymers and blends were determined by differential scanning calorimetry (DSC, Perkin-Elmer) at a heating rate of 10 K min^{-1}. The homopolymers show T_g values of 312 K (PVAc) and 206 K (PEO). The blend samples with 5, 10 and 20% PEO concentrations show T_g values of 303, 294 and 280 K, respectively.

The mechanical spectroscopy measurements were conducted on a modified low-frequency inverted torsion pendulum with a Couette-like setup using the forced-vibration method.[44] The apparatus consists of the traditional torsion shaft equipped with two co-axial cylindrical cells for liquid samples. In the measurements, the inner cylinder is forced into torsional vibration by a time-dependent force $F(t) = F_0\sin(\omega t)$, where ω is the measurement circular frequency. The angular displacement function of the cylinder, $A(t)$, is measured optically. In the case here, the response of the argument can be expressed as $A(t) = A_0\sin(\omega t - \phi)$, where ϕ is the phase difference between $F(t)$ and $A(t)$. The mechanical loss of the oscillating system, characterized by Q^{-1}, is given by

$$Q^{-1} = \frac{1}{2\pi}\frac{\Delta W}{W} = \frac{1}{2\pi}\frac{\int FdA}{\int_0^{\pi/2} dW - \frac{1}{4}\Delta W} = \frac{1}{2\pi}\frac{F_0A_0\pi\sin\phi}{1/2\,F_0A_0\cos\phi} = \tan\phi \quad (1)$$

where ΔW and W are the dissipated energy and the maximum stored energy per cycle, respectively.

In the measurement, the mechanical loss (tanϕ) and the relative modulus ($G = F_0/A_0$) were measured over a frequency range 5×10^{-3} to 100 Hz for each of the temperatures at which the sample was isothermally kept. In our experiments, isothermal measurements were first carried out at low temperatures and thereafter the isothermal spectra were measured at predetermined temperature intervals by increasing the sample's temperature in steps. G and tanϕ of the sample were also measured over a temperature range 300–470 K at fixed frequencies of 0.1, 0.5, and 2.0 Hz. In all tests, the samples were protected by argon with a pressure of 0.1 MPa to avoid oxidation and degradation.

In frequency domain, the response function is broader than that corresponding to a Debye process (1.14 decades width at half maximum). This width has been modelled by many empirical functions.[45] Among them, the model function proposed by Cole and Cole[46] has been extensively used,[47,48] and the function for the complex modulus (G^*) is defined as:

$$G^*(\omega) = G'(\omega) + iG''(\omega) = G_\infty - \frac{G_\infty - G_0}{1 + (i\omega\tau)^\beta} \quad (2)$$

where G_0 and G_∞ denote the rubbery regime modulus in the low-frequency limit and the glassy regime modulus in the high-frequency limit, respectively. Accordingly, the frequency-domain

mechanical relaxation spectra can be analyzed by fitting the mechanical loss peaks using a modified Debye equation,[47,48]

$$\tan\phi = \frac{(1/2)\Delta\sin(\beta\pi/2)}{\cosh(\beta z) + \cos(\beta\pi/2)} \quad (3)$$

where Δ is the relaxation strength, $z = \ln(\omega\tau)$, and β ($0 < \beta \leq 1$) is the width parameter leading to a symmetric broadening of the Debye relaxation ($\beta = 1$ corresponds to the standard Debye relaxation). The conversion of the Havriliak–Negami (HN) exponent to the stretching parameter β_{KWW} has been studied and here for the Cole–Cole (CC) function $\beta_{KWW} = \beta^{1/1.23}$.[49,50]

For a single Debye relaxation processes, the mechanical loss peak occurs at the following condition,[51]

$$\omega\tau(T_p) = 1 \quad (4)$$

where τ is the relaxation time. In thermally activated processes, the peak shifts to higher temperature with increasing frequency with a relaxation time following an Arrhenius type equation,

$$\tau = \tau_0 \exp(H/k_B T_p) \quad (5)$$

where τ_0 is a preexponential factor, k_B is the Boltzmann constant, and H is the activation energy. For the relaxation near and above T_g, the relaxation time exhibits a deviation from simple Arrhenius behavior and it is usually described by the so-called Vogel–Fulcher–Tamman (VFT) equation,

$$\tau = \tau_\infty \exp\left[\frac{B}{k_B(T - T_0)}\right] \quad (6)$$

where τ_∞ is the preexponential factor, T_0 is the critical temperature (or "Vogel temperature") at which the relaxation time diverges to infinity, and B is the so-called Vogel activation energy.

Results and discussion

Fig. 1(a) and 1(b) show the mechanical spectra (tanϕ and G) of pure PVAc and the PEO/PVAc blend with 10% PEO at three different frequencies in the temperature range 300–470 K. The mechanical loss exhibits an asymmetrical broad peak with a shoulder at the low temperature side for the pure PVAc and the blend. The asymmetrical structure could be well fitted by two peaks (α and α' peaks) with distributions in relaxation time using a nonlinear fitting method.[52,53] The details of the fitting results are given only at 0.5 Hz for clarity, as shown in Fig. 1. Obviously, two relaxation mechanisms are responsible for the α and α' peaks, and the corresponding processes are described as the α and α' modes for simplicity.

Since the minimum temperatures of the α peaks agree approximately with the T_g values of PVAc and the blend determined by DSC measurements, the α peak is associated with the local segmental mode of PVAc and is known to be ascribed to the cooperative rearrangement of chain segments when T_g is approached.[54] The local segmental motion usually involves correlated local motion of only a few backbone bonds. On the other hand, the α' peak should be attributed to the motion of longer chain segments because they are expected to move at a higher temperature.[55] Compared with the creep behavior of

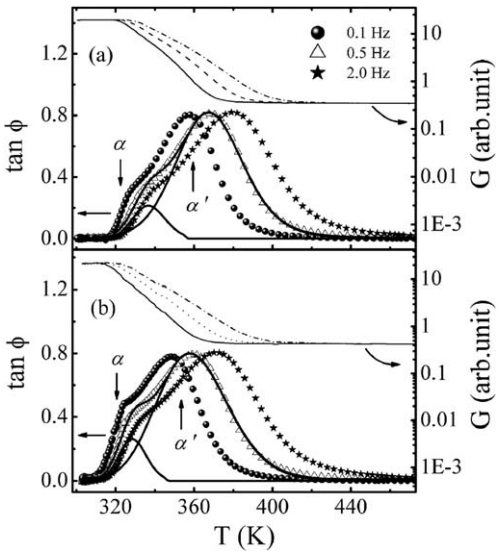

Fig. 1 Mechanical loss and relative modulus measured at three vibration frequencies of (a) PVAc, and (b) blend with 10/90 PEO/PVAc. Solid lines are the fitting of the α and α' peaks at 0.5 Hz. Two peaks appear explicitly.

PVAc,[25] it is reasonable to associate the α' mode with the softening dispersion of PVAc composed of the sub-Rouse modes and the Rouse modes, which usually involves the motion of chain segments containing about 10 to 50 or more backbone bonds.[27] Moreover, the main tanϕ peak mainly reflects the sub-Rouse mode and Rouse mode.[36,37] This explains why the value of tanϕ of the α' mode is so much larger than that of the α mode. The sub-Rouse modes have been reflected by many experimental techniques such as mechanical spectroscopy, photo correlation spectroscopy and dielectric relaxation spectroscopy.[30,56,57]

It can be also observed that the two modes have different frequency shift factors. The α' mode exhibits a stronger frequency dependence than the α mode.[27,28] For example, as the frequency varies from 2 Hz to 0.1 Hz for the blend (Fig. 1b), the α peak shifts from about 327 K to 319 K with a interval of 8 K; however, the α' peak shifts from 372 K to 347 K with a larger interval of 25 K. So the α' peak moves faster to lower temperature than the α peak with decreasing frequency. As a result, the α peak is almost overlapped by the α' peak at low frequencies due to the merging of the α' peak with the α peak. A similar phenomenon has also been observed in poly(methyl methacrylate) and chlorinated butyl rubber.[55,58] In the opposite way, the relaxation time of the α mode is more sensitive to temperature than that of the α' mode. This is understandable because the strongly coupled polymers such as PVAc and polystyrene (PS) exhibit a temperature dependence of their local segmental relaxation that is much stronger than the sub-Rouse modes and Rouse modes.[26,29] As temperature is lowered toward T_g, the local segmental motion encroaches into the time scale of the α' mode. The fact that the α and α' modes have distinct temperature dependencies also means that each of them can be associated with a different friction factor.

Fig. 2 shows the mechanical spectra (tanϕ and G) for pure PVAc and PEO/PVAc blends with different PEO concentrations at 2 Hz. Similarly, the blends exhibit the asymmetrical loss peak

that could be well fitted by the α and α′ peaks using the nonlinear fitting method. The details of the fitting results are given only for pure PVAc and 10/90 PEO/PVAc blend for clarity. The arrow in the figure positions the α and α′ relaxations of PVAc and the blends. The outstanding feature in Fig. 2 is the trend of variations of mechanical loss. As observed, both the α and α′ peaks shift to low temperatures with an increasing amount of PEO in the blend. It is known that the peak temperature of the relaxation partly reflects the rotational or reptational energy barriers in the chains, with a lower transition temperature indicating a lower energy barrier.[59] The decreasing energy barriers induced by the addition of PEO above T_g leads to a drastic increase in molecular mobility. Thus, PEO plays a plasticizer-like role in the softening dispersion, increasing the free volume fraction to enhance the PVAc chain mobility. On the other hand, with increasing PEO content in the blend, damping factor does not show a monotonic behavior. The damping factor is increased with addition of PEO to PVAc up to 5%, but it is decreased for blends containing 10% and 20% PEO. The damping factor is firstly increased since more PVAc chains can relax due to the large free volume induced by PEO. However, it is expected that addition of higher amount of PEO (low damping component) to PVAc (high damping component) results in a decrease in damping factor of the blend.

Fig. 3 exhibits the frequency-domain mechanical spectra of the 10/90 PEO/PVAc blend at different temperatures above T_g. The tanϕ peak in Fig. 3 is associated with the α′ mode in comparison with Fig. 2. The frequency f_m at which tanϕ takes the maximum value shifts to higher frequency with increasing temperature (Fig. 3b), indicating the increasing mobility of chain segments at higher temperatures. By fitting the tanϕ peak with eqn (3), the α′ mode is obtained where the background may consist of the damping of the high-frequency α relaxation and the intrinsic damping of the apparatus, as shown in Fig. 3b.

TTS is the basic principle widely used for analysis of dynamics of supercooled liquids and polymers, expressing the fact that the shape of the response function remains the same when the system is cooled.[60–62] The validity of TTS refers to the situation where the increase (or decrease) of temperature moves only the time scale of the mechanical response and does not affect the shape of the loss peak. A normalized master curve of the loss data for one example of PEO/PVAc blends above T_g is plotted in Fig. 4a. Similar to pure PVAc,[35] the TTS principle is invalid for PEO/PVAc blends in the entire temperature range, which may be due to the different friction coefficients of the α and α′ modes. It can be also observed that the α′ relaxation peak is broader than that for classical Debye response. The normalized data of the α′ mode at different compositions are compared at T_g + 68 K in Fig. 4b. The width of the α′ mode is not appreciably influenced by blending, at least in the temperature range here investigated. This feature reflects that blending does not affect the relaxation time distribution and the movement environment of relaxing species for the α′ mode.

As the temperature is lowered toward T_g, the relaxation times of amorphous polymers change strongly, and the temperature

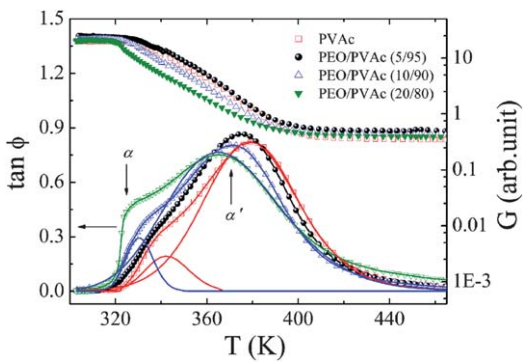

Fig. 2 Temperature dependence of mechanical spectra (tanϕ and G) for pure PVAc and PEO/PVAc blends with three different compositions at 2 Hz. Arrows show the α and α′ relaxations of PVAc and the blends. The solid lines are the fitting of the α and α′ peaks for pure PVAc and the blend with 10% PEO.

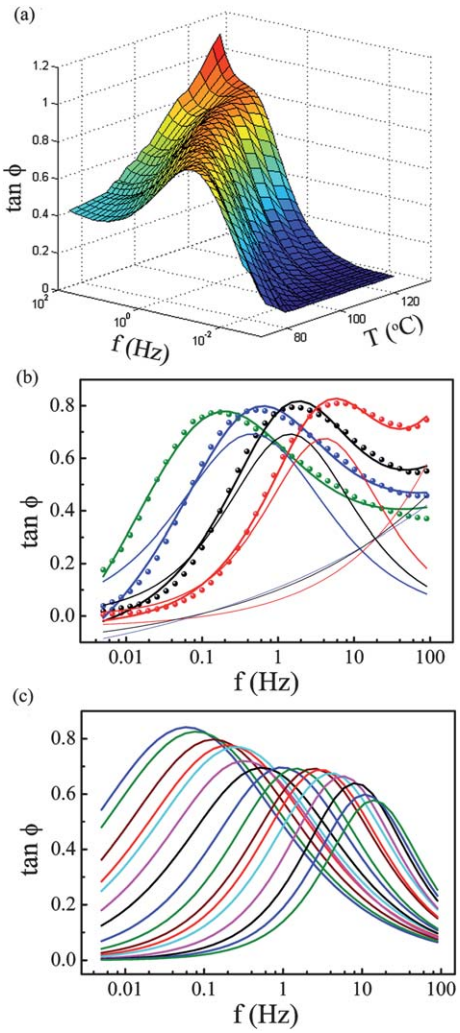

Fig. 3 Mechanical relaxation behavior of the blend with 10/90 PEO/PVAc above T_g: (a) 3D plot of the temperature and frequency dependencies of mechanical loss tanϕ; (b) tanϕ at the temperatures (from left to right): 353.5, 363.2, 372.5, and 384.5 K, where the symbols are experimental data points and the solid lines are the total fitting results. The fitting peak and the corresponding fitting background are down for the results at 363.2, 372.5, and 384.5 K. (c) The fitting mechanical loss peak at the temperatures (from left to right): 347.5, 350.5, 353.5, 356, 359, 361.5, 364.6, 369, 372.5, 377.5, 380.5, 384.5, 388, 396.5, 404, and 409 K.

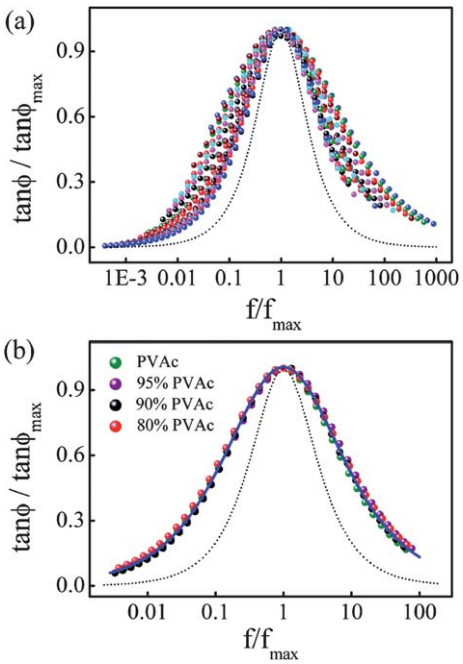

Fig. 4 (a) The normalized master curves for the α' mode of the blend with 20/80 PEO/PVAc at the temperatures (from outside to inside): 343.5, 347.5, 351.5, 355.4, 358.2, 361.5, 363.5, 368.2, 371, 373.5, 376.5, 378.4, 379.4, 380, 382, 383.5, 386.5, 389.5, 392.8, 397.5, 401.5, and 405 K. (b) Normalized loss curves for the α' mode of pure PVAc and the blends at T_g + 68 K. The dotted lines in (a) and (b) represent the standard Debye peak.

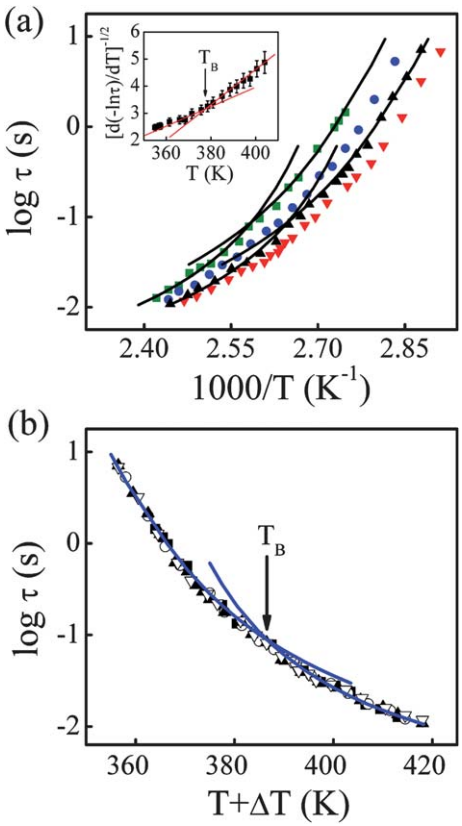

Fig. 5 Relaxation map of pure PVAc and PEO/PVAc blends. (a) Temperature dependence of relaxation time of the α' mode for pure PVAc and PEO/PVAc blends with different PEO weight fractions: (■) 0, (●) 5, (▲) 10, and (▼) 20% PEO. Two VFT equations are required to describe the relaxation behavior of pure PVAc and PEO/PVAc blends. The solid lines represent the two VFTs for pure PVAc and the blend with 10/90 PEO/PVAc. The inset shows the plots of $[d(-\ln\tau)/dT]^{-1/2}$ against temperature for 10/90 PEO/PVAc blend. The intersection of two solid lines which correspond to two VFTs shown in this figure denotes the crossover temperature T_B = 378 K. (b) To construct this single curve, pure PVAc data were fixed and the blend data were shifted. The solid lines which represent two best-fit VFT curves for pure PVAc could also describe approximately the T-dependent relaxation time of the α' mode for PEO/PVAc blends.

dependence of relaxation times $\tau(T)$ in these systems deviates strongly from a simple thermally activated behavior or Arrhenius behavior. The strong non-Arrhenius character of the dynamics of the α' mode in pure PVAc and the blends can be seen from Fig. 5a where logτ against $1/T$ is plotted from the fitting of tanϕ peak with eqn (3). Usually, an excellent representation of the $\tau(T)$ dependence could be described by the VFT equation. However, a close examination of the data over a wide temperature range where the α' mode occurs reveals that the $\tau(T)$ dependence cannot be described accurately by a single VFT equation over the entire temperature range and two VFT equations are required. The first equation describes well the $\tau(T)$ dependence only up to the crossover temperature T_B. At this temperature the dynamic crossover occurs and for temperatures $T > T_B$ another VFT equation is needed. In our previous work,[35] we have shown that the α' mode of PVAc exhibited a similar dynamic crossover as the α mode, where the crossover of the α mode was due to the strong increase of intermolecular cooperativity and could be observed for most of the conventional glass-formers and polymers.[63–70] However, the crossover relaxation time of the α' mode is about 0.08 s, much longer than $10^{-7\pm1}$ s for the α mode.[63,64] To estimate T_B in PEO/PVAc blends we applied distortion-sensitive derivative based analysis.[66] For the VFT equation the following formula is given

$$[d(-\ln\tau)/dT]^{-1/2} = \left(\frac{B}{k_B}\right)^{-1/2}(T - T_0) \quad (7)$$

Hence, by plotting $[d(-\ln\tau)/dT]^{-1/2}$ *versus* T in the domain of validity of the VFT equation, the experimental data should follow a linear dependence. The result of such an analysis is shown only for 10/90 PEO/PVAc blend, where it can be seen that $[d(-\ln\tau)/dT]^{-1/2}$ *versus* T for the blend is not linear over the entire temperature range (the inset of Fig. 5a). Data well below 378 K lie on one straight line, and data well above 378 K lie on another. Assuming that the functional forms of $\tau(T)$ are the same for all the blend compositions, we superposed the τ data of the blends to that of pure PVAc with the shift in the direction of the T axis and the result is shown in Fig. 5b. The shifted temperatures ΔT represent the difference of transition temperatures of the α' mode ($T_{\alpha'}$) so that $T_{\alpha'}$ can be determined from the simple equation:

$$T_{\alpha'} = T_{\alpha'}(\text{PVAc}) - \Delta T \quad (8)$$

Here at 2.0 Hz, $T_{\alpha'}$(PVAc) = 380 K and the $T_{\alpha'}$ values for the PEO/PVAc blends could be obtained from Fig. 2. According to ref. 40, the local segmental dynamics of the PVAc component in

PEO/PVAc blends does not change with blending. Therefore, both the α and α′ relaxation modes could each be represented by a single curve, although they have different T dependences. The values of these obtained VFTs for the blends agree with those of pure PVAc.[35] This means that blending does not alter the size of chain segments from only a few backbone bonds to Gaussian sub-molecules. The addition of PEO leads to a drastic increase in molecular mobility, so the energy barriers of movement of backbone bonds and Gaussian sub-molecules are decreased. As a result, T_B decreases with increasing PEO content.

The crossover of the α′ mode of the blends is also shown in the variation of relaxation strength Δ. Fig. 6 exhibits the temperature dependence of Δ of pure PVAc and the blends. The dynamic crossover is shown for all the samples. Note that above T_B, Δ decreases slowly with increasing temperature. Generally, Δ of a cooperative relaxation decreases due to the decreased cooperativity because of the enhanced thermal energy with increasing temperature.[5,71] Thus, the change in Δ with temperature can be a useful tool for indicating the extent of cooperativity of α′ relaxation. The fact that Δ is a decreasing function of temperature suggests the decreased cooperativity of the α′ mode.

The relaxation strength Δ and the relaxation time τ reflect different properties of the same underlying motional process, and hence both should be correlated in their temperature dependence.[72] In Fig. 7 we have plotted the relaxation strength of 10/90 PEO/PVAc blend against logτ to see any such correlations. The diagram can easily be separated into two regions where the Δ variation against logτ can be described by two separate straight lines. The intersection of two lines leads to a crossover relaxation time of nearly 0.08 s which corresponds to $\tau_0(T_B)$ of the α′ mode obtained from the VFT analysis. It is apparent that Δ increases as a function of logτ much more rapidly in the regime $T > T_B$ than for $T < T_B$, consistent with the crossover at T_B in Fig. 5.

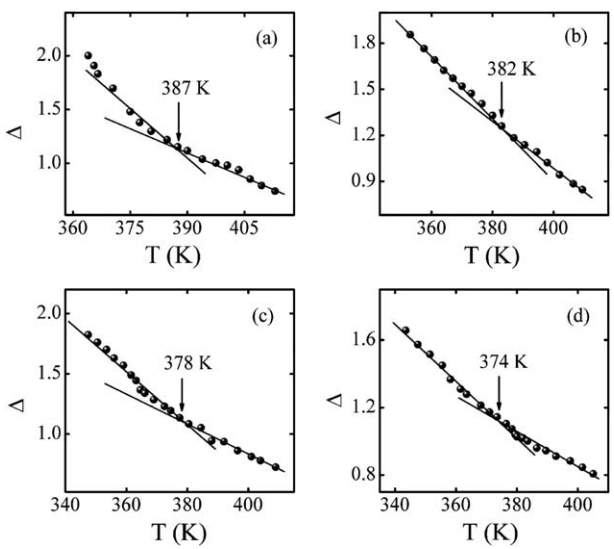

Fig. 6 Temperature dependence of relaxation strength Δ for pure PVAc (a) and PEO/PVAc blends with different PEO weight fractions: (b) 5, (c) 10, and (d) 20% PEO. The solid lines are a guide to the eyes. The crossover temperature T_B is apparent from the change in T dependence of Δ and its value decreases with increasing PEO content.

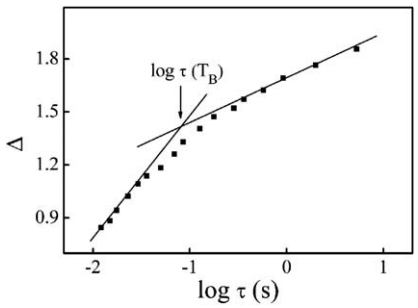

Fig. 7 Variation of the relaxation strength Δ of the α′ mode of 10/90 PEO/PVAc blend against characteristic relaxation times in log scales. The marked increase of Δ reveals the crossover at T_B.

In the present study we show that the sub-Rouse modes of the PVAc component in the blends exhibit a similar dynamic crossover through the change of T-dependence in relaxation time and relaxation strength. As described above, the sub-Rouse modes have a smaller intermolecular coupling than that of the local segmental mode. The CM is appropriate for describing this kind of intermolecular coupling and can explain the experimental data of the sub-Rouse modes.[28,73] The basis of the CM is the putative existence of a temperature-insensitive crossover time, t_c, equal to about 2 ps for molecular liquids. According to the CM, the correlation function $\phi(t)$ is very different in two regions separated by t_c. That is, for $t < t_c$,

$$\phi(t) = \exp[-(t/\tau^*)] \quad (9)$$

and for $t > t_c$,

$$\phi(t) = \exp[-(t/\tau)^{1-n}] \quad (10)$$

Here τ and τ* are the relaxation time measured experimentally and the primitive (non-cooperative) relaxation time, while n ($0 \leq n < 1$) is the coupling parameter that provides a measure of the degree of intermolecular coupling. In the CM, n increases with increasing molecular interaction strength and comparisons of the values of n for different glass-formers at their respective T_g reveals differences in intermolecular coupling strength. The temperature dependence of n also reflects how intermolecular coupling changes with temperature. Since the parameter n is equivalent to $(1 - \beta_{KWW})$ by Fourier transformation[74] and for the CC function $\beta_{KWW} = \beta^{1/1.23}$ as mentioned above, the value of n is approximately equal to $(1 - \beta)$. Therefore, we could calculate the parameter n by fitting the frequency domain mechanical spectra with eqn (3). Fig. 8 shows the temperature variation of n of pure PVAc and PEO/PVAc blends. It can be seen that for all the samples, with decreasing temperature, the crossover at T_B from a slowly varying and small value of n to a rapid increase of n towards a large value approaching T_g supports the interpretation of substantial intermolecular cooperativity arising below T_B in PVAc. Therefore, the crossover is suggested to be due to the change of the intermolecular coupling at T_B. On the other hand, there is no indication of dynamic crossover for the chain relaxation or terminal relaxation.[63,64,69] There are two possible reasons for this observation. First the entanglement coupling is constant, unlike the coupling for segmental relaxation and sub-Rouse

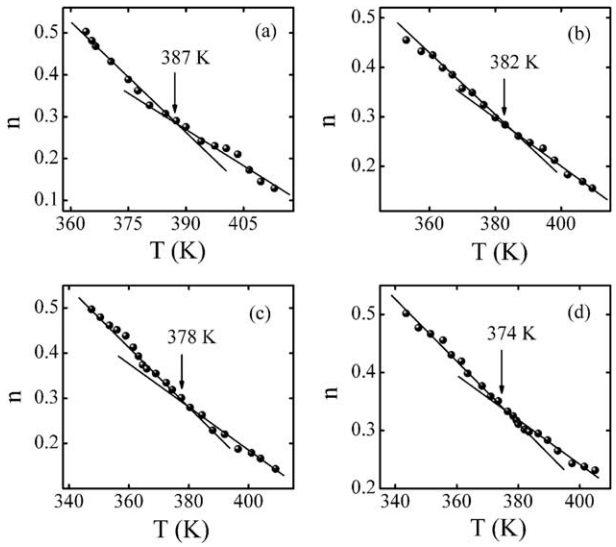

Fig. 8 Temperature dependence of coupling parameter n for pure PVAc (a) and PEO/PVAc blends with different PEO weight fractions: (b) 5, (c) 10, and (d) 20% PEO. The solid lines are a guide to the eyes. The change in T dependence of n denotes the crossover temperature T_B at (a) 387 K, (b) 382 K, (c) 378 K, and (d) 374 K, respectively.

modes. The second reason is the much longer time of the terminal relaxation for entangled polymers. If the crossover for the terminal relaxation time exists also at T_B, it will be much longer and cannot be easily observed.

In the previous mechanical and dielectric measurements of amorphous polymers, the α' mode is usually thought of as the so-called "liquid–liquid transition" (T_{ll}),[75–77] although the rubbery–viscous transition may be a more appropriate label.[78] T_{ll} is considered as a molecular level relaxation associated with thermal disruption of segment–segment contacts, and has been observed in many amorphous polymers and copolymers.[75,79] The temperatures of T_g and T_{ll} vary congruously as a function of copolymer composition and there is a well-defined relationship, $T_{ll} = 1.2\ T_g$, between T_g and T_{ll}.[79] The value of T_{ll}/T_g is in agreement with the observation for T_B/T_g ratio. Murthy[80] has assigned the dynamic crossover to be the liquid–liquid transition. Contrarily, Kisliuk *et al.*[81] believed that the crossover is dynamic in origin and is strongly different from thermodynamic liquid–liquid transition. On the other hand, the occurrence of T_{ll} is discredited by Plazek and co-workers[82] and there is no transition in the softening dispersion zone. Here, we prove that no sign of thermodynamic transition appears and the only change is the variation of the intermolecular coupling at T_B. The value of T_B decreases with increasing PEO content and the ratio T_B/T_g is about 1.2 and essentially independent of blend compositions, whereas the crossover relaxation time of the α' mode for the blends is constant with a value about 0.08 s (Fig. 5).

Conclusions

In this paper by means of mechanical spectroscopy we have studied the longer-scale segmental dynamics of the PVAc component in PEO/PVAc blends covering wide temperature and frequency range. Two relaxation modes were observed: the α mode is related to the local segmental mode, while the α' mode is assigned to the softening dispersion composed of the sub-Rouse modes and Rouse modes. The local segmental mode has a stronger temperature dependence of relaxation time than the sub-Rouse modes and Rouse modes. PEO plays a plasticizer-like role in the softening dispersion, increasing the free volume fraction to enhance the PVAc chain mobility and leading to lower transition temperatures of the α and α' modes at a higher PEO concentration.

Similar to pure PVAc, the α' mode of PVAc component in the blends is found to show a characteristic crossover in the dynamics through the temperature dependence of relaxation time and relaxation strength. The influence of blending on the PVAc component can be considered as "standard", which does not alter the size of chain segments from only a few backbone bonds to Gaussian sub-molecules, and just only decreases the energy barrier of chain segment motion. So a single master curve of the α' mode for pure PVAc and the PEO/PVAc blends is obtained, and the crossover temperature T_B decreases with increasing PEO content. The application of the coupling model to the data suggests that this crossover is due to the variation of intermolecular coupling at T_B.

Acknowledgements

The financial support of National Natural Science Foundation of China (50803066, 10874182 and 10674135) is gratefully acknowledged.

References

1 S. Hoffmann, L. Willner, D. Richter, A. Arbe, J. Colmenero and B. Farage, *Phys. Rev. Lett.*, 2000, **85**, 772.
2 D. Lumma, M. A. Borthwick, P. Falus, L. B. Lurio and S. G. J. Mochrie, *Phys. Rev. Lett.*, 2001, **86**, 2042.
3 B. Farago, C. X. Chen, J. K. Maranas, S. Kamath, R. H. Colby, A. J. Pasquale and T. E. Long, *Phys. Rev. E: Stat., Nonlinear, Soft Matter Phys.*, 2005, **72**, 031809.
4 Y. Y. He, T. R. Lutz and M. D. Ediger, *J. Chem. Phys.*, 2003, **119**, 9956.
5 X. Jin, S. H. Zhang and J. Runt, *Macromolecules*, 2003, **36**, 8033.
6 X. Jin, S. H. Zhang and J. Runt, *Macromolecules*, 2004, **37**, 8110.
7 J. Colmenero and A. Arbe, *Soft Matter*, 2007, **3**, 1474.
8 K. L. Ngai and C. M. Roland, *Rubber Chem. Technol.*, 2004, **77**, 579.
9 Y. Hirose, O. Urakawa and K. Adachi, *Macromolecules*, 2003, **36**, 3699.
10 H. Watanabe and O. Urakawa, *Korea-Aust. Rheol. J.*, 2009, **21**, 235.
11 S. Kamath, R. H. Colby and S. K. Kumar, *Macromolecules*, 2003, **36**, 8567.
12 S. S. Es-Haghi, A. A. Yousefi and A. Oromiehie, *J. Polym. Sci., Part B: Polym. Phys.*, 2007, **45**, 2860.
13 A. Zetsche and E. W. Fischer, *Acta Polym.*, 1994, **45**, 168.
14 G. Katana, E. W. Fischer, T. Hack, V. Abetz and F. Kremer, *Macromolecules*, 1995, **28**, 2714.
15 S. K. Kumar, R. H. Colby, S. H. Anastasiadis and G. Fytas, *J. Chem. Phys.*, 1996, **105**, 3777.
16 S. Kamath, R. H. Colby, S. K. Kumar, K. Karatasos, G. Floudas, G. Fytas and J. E. L. Roovers, *J. Chem. Phys.*, 1999, **111**, 6121.
17 S. Salaniwal, R. Kant, R. H. Colby and S. K. Kumar, *Macromolecules*, 2002, **35**, 9211.
18 S. Kamath, R. H. Colby and S. K. Kumar, *Phys. Rev. E: Stat., Nonlinear, Soft Matter Phys.*, 2003, **67**, 010801.
19 T. P. Lodge and T. C. B. McLeish, *Macromolecules*, 2000, **33**, 5278.
20 J. S. Zhao, L. Zhang and M. D. Ediger, *Macromolecules*, 2008, **41**, 8030.
21 K. L. Ngai and C. M. Roland, *Macromolecules*, 2004, **37**, 2817.

22 E. Leroy, A. Alegría and J. Colmenero, *Macromolecules*, 2003, **36**, 7280.
23 R. H. Colby and J. E. G. Lipson, *Macromolecules*, 2005, **38**, 4919.
24 S. Shenogin, R. Kant, R. H. Colby and S. K. Kumar, *Macromolecules*, 2007, **40**, 5767.
25 D. J. Plazek, *Polym. J.*, 1980, **12**, 43.
26 P. G. Santangelo, K. L. Ngai and C. M. Roland, *Macromolecules*, 1993, **26**, 2682.
27 D. J. Plazek, I. C. Chay, K. L. Ngai and C. M. Roland, *Macromolecules*, 1995, **28**, 6432.
28 K. L. Ngai, D. J. Plazek and A. K. Rizos, *J. Polym. Sci., Part B: Polym. Phys.*, 1997, **35**, 599.
29 K. L. Ngai, D. J. Plazek and R. W. Rendell, *Rheol. Acta*, 1997, **36**, 307.
30 M. Paluch, S. Pawlus, A. P. Sokolov and K. L. Ngai, *Macromolecules*, 2010, **43**, 3103.
31 J. M. Pelletier, C. Gauthier and L. Chazeau, *Int. J. Materials and Product Technology*, 2006, **26**, 312.
32 T. Haramina and R. Kirchheim, *Macromolecules*, 2007, **40**, 4211.
33 C. Castellano, J. Generosi, A. Congiu and R. Cantelli, *Appl. Phys. Lett.*, 2006, **89**, 233905.
34 X. B. Wu, S. Y. Shang, Q. L. Xu, C. S. Liu, Z. G. Zhu and G. Z. Zhang, *Appl. Phys. Lett.*, 2008, **93**, 011910.
35 X. B. Wu and Z. G. Zhu, *J. Phys. Chem. B*, 2009, **113**, 11147.
36 E. Donth, M. Beiner, S. Reissig, J. Korus, F. Garwe, S. Vieweg, S. Kahle, E. Hempel and K. Schroter, *Macromolecules*, 1996, **29**, 6589.
37 K. L. Ngai and D. J. Plazek, *Rubber Chem. Technol.*, 1995, **68**, 376.
38 M. Tyagi, A. Arbe, J. Colmenero, B. Frick and J. R. Stewart, *Macromolecules*, 2006, **39**, 3007.
39 M. Tyagi, A. Arbe, A. Alegria, J. Colmenero and B. Frick, *Macromolecules*, 2007, **40**, 4568.
40 O. Urakawa, T. Ujii and K. Adachi, *J. Non-Cryst. Solids*, 2006, **352**, 5042.
41 D. Fragiadakis and J. Runt, *Macromolecules*, 2010, **43**, 1028.
42 L. H. Sperling, *Introduction to Physical Polymer Science*, Wiley, New Jersey, 4th edn, 2006, p. 537.
43 L. J. Fetters, D. J. Lohse and R. H. Colby, in *Physical Properties of Polymers Handbook*, ed. J. E. Mark, Springer, New York, 2nd edn, 2006, p. 451.
44 X. B. Wu, Q. L. Xu, J. P. Shui and Z. G. Zhu, *Rev. Sci. Instrum.*, 2008, **79**, 126105.
45 P. A. Beckmann, *Phys. Rep.*, 1988, **171**, 85.
46 K. S. Cole and R. H. Cole, *J. Chem. Phys.*, 1941, **9**, 341.
47 C. Ang, Z. Yu and L. E. Cross, *Phys. Rev. B: Condens. Matter Mater. Phys.*, 2000, **62**, 228.
48 X. P. Wang and Q. F. Fang, *Phys. Rev. B: Condens. Matter Mater. Phys.*, 2002, **65**, 064304.
49 C. P. Lindsey and G. D. Patterson, *J. Chem. Phys.*, 1980, **73**, 3348.
50 F. Alvarez, A. Alegria and J. Colmenero, *J. Phys. Chem. B*, 1993, **47**, 125.
51 A. S. Nowick and B. S. Berry, *Anelastic Relaxation in Crystalline Solids*, Academic, New York, 1972.
52 L. X. Yuan and Q. F. Fang, *Acta Met. Sinica*, 1998, **34**, 1016.
53 X. P. Wang and Q. F. Fang, *J. Phys.: Condens. Matter*, 2001, **13**, 1641.
54 E. Munch, J. M. Pelletier, B. Sixou and G. Vigier, *Phys. Rev. Lett.*, 2006, **97**, 207801.
55 J. R. Wu, G. S. Huang, Q. Y. Pan, J. Zheng, Y. C. Zhu and B. Wang, *Polymer*, 2007, **48**, 7653.
56 K. L. Ngai and D. J. Plazek, *Macromolecules*, 2002, **35**, 9136.
57 A. K. Rizos, K. L. Ngai and D. J. Plazek, *Polymer*, 1997, **38**, 6103.
58 X. B. Wu, X. M. Zhou, C. S. Liu and Z. G. Zhu, *J. Appl. Phys.*, 2009, **106**, 013527.
59 J. Wu, T. S. Haddad, G. M. Kim and P. T. Mather, *Macromolecules*, 2007, **40**, 544.
60 Y. Ding and A. P. Sokolov, *Macromolecules*, 2006, **39**, 3322.
61 D. J. Plazek, *J. Non-Cryst. Solids*, 2007, **353**, 3783.
62 C. Maggi, B. Jakobsen, T. Christensen, N. B. Olsen and J. C. Dyre, *J. Phys. Chem. B*, 2008, **112**, 16320.
63 K. L. Ngai and C. M. Roland, *Polymer*, 2002, **43**, 567.
64 M. Tyagi, A. Alegria and J. Colmenero, *J. Chem. Phys.*, 2005, **122**, 244909.
65 A. Schönhals, F. Kremer, A. Hofmann, E. W. Fischer and E. Schlosser, *Phys. Rev. Lett.*, 1993, **70**, 3459.
66 F. Stickel, E. W. Fischer and R. Richert, *J. Chem. Phys.*, 1995, **102**, 6251.
67 C. M. Roland, *Soft Matter*, 2008, **4**, 2316.
68 V. N. Novikov and A. P. Sokolov, *Phys. Rev. E: Stat., Nonlinear, Soft Matter Phys.*, 2003, **67**, 031507.
69 S. Pawlus, K. Kunal, L. Hong and A. P. Sokolov, *Polymer*, 2008, **49**, 2918.
70 R. Casalini, K. L. Ngai and C. M. Roland, *Phys. Rev. B: Condens. Matter Mater. Phys.*, 2003, **68**, 014201.
71 A. Schönhals, in *Dielectric Spectroscopy of Polymer Materials: Fundamentals and Applications*, ed. J. P. Runt and J. J. Fitzgerald, American Chemical Society, Washington, DC, 1997, p. 107.
72 A. Schönhals, *Europhys. Lett.*, 2001, **56**, 815.
73 K. L. Ngai, in *Disorder Effects on Relaxation Porcess*, ed. R. Richert and A. Blumer, Springer, Berlin, 1994.
74 D. Prevosto, S. Capaccioli, M. Lucchesi, P. A. Rolla and K. L. Ngai, *J. Chem. Phys.*, 2004, **120**, 4808.
75 D. Park, B. Keszler, V. Galiatsatos and J. P. Kennedy, *J. Appl. Polym. Sci.*, 1997, **66**, 901.
76 E. Dudognon, A. Bernès and C. Lacabanne, *Macromolecules*, 2002, **35**, 5927.
77 E. Dudognon, A. Bernès and C. Lacabanne, *Polymer*, 2002, **43**, 5175.
78 S. Hedvat, *Polymer*, 1981, **22**, 774.
79 P. L. Kumler, G. A. Machajewshi, J. J. Fitzgerald, L. R. Denny, S. E. Keinath and R. F. Boyer, *Macromolecules*, 1987, **20**, 1060.
80 S. S. N. Murthy, *J. Polym. Sci., Part B: Polym. Phys.*, 1993, **31**, 475.
81 A. Kisliuk, R. T. Mathers and A. P. Sololov, *J. Polym. Sci., Part B: Polym. Phys.*, 2000, **38**, 2785.
82 D. J. Plazek, *J. Polym. Sci., Part B: Polym. Phys.*, 1982, **20**, 1533.

